On energy exchanges in hypersonic flows

Yitong Fan and Weipeng Li*

School of Aeronautics and Astronautics, Shanghai Jiao Tong University, Shanghai, China, 200240

Sergio Pirozzoli

Dipartimento di Ingegneria Meccanica e Aerospaziale,
Sapienza Università di Roma, Via Eudossiana 18, Roma, Italy, 00184

(Dated: August 7, 2022)

We present a new framework to quantitatively describe energy exchange in high-speed turbulent flows, also including the hypersonic regime. Governing equations are introduced which control the transport of the mean-field kinetic energy (k_m), the turbulence kinetic energy (k_t), the mean-field internal energy (e_m), and the turbulence internal energy (e_t). The common terms in the transport equations are found to represent energy exchanges and interactions among k_m, k_t, e_m, and e_t. The routes of energy exchange are then highlighted and quantified in hypersonic boundary-layer flow, with special attention paid to effects of wall cooling.

Introduction.—Energy, which is a fundamental property in nature, may exist in different sensible forms within a perfect heat-conducting gas, such as kinetic and internal energy. Energy exchanges between kinetic and internal energy are known to play a leading role in aerodynamics and thermodynamics [1–3].

Several studies have investigated the transport of kinetic energy in incompressible turbulent flows [4–6], in which the internal energy is a constant and the conversion between the kinetic and internal energy is only attributed to the viscous work. In compressible flows processes of energy transformation are more complicated [1, 2], on account of density variation and finite dilatation, and especially in hypersonic boundary layers, where the wall temperature is usually lower than the recovery temperature of the free-stream flow. A growing body of studies has investigated the flow dynamics of hypersonic boundary layers over cold walls [7–10], and the results have shown that both flow speed (as expressed by the Mach number) and wall cooling can affect the mean and fluctuation properties significantly [11, 12]. In particular, it is known that the mean temperature gradient flips its sign over cold walls, which challenges the validity of traditional modeling approaches based on mapping to an equivalent incompressible flow [13–16]. Wall cooling acts to strengthen energy exchanges between kinetic and internal energy [17], which are associated with the action of pressure. To date, very few studies have focused on energy exchanges in hypersonic turbulent boundary layers and shed light on the underlying physical processes.

This letter reports on a full set of transport equations for describing routes of energy exchanges in compressible flows, which we use to scrutinize hypersonic turbulent boundary layers with/without wall-cooling.

The Database.—Two direct numerical simulations (DNS) of spatially-developing zero-pressure-gradient hypersonic turbulent boundary layers have been performed, with common free-stream Mach number $M_0 = 5.86$, and with wall-to-recovery temperature ratio T_w/T_r set to 1.0 and 0.25, signifying adiabatic and cold wall conditions, respectively. A well validated solver [18] of the three-dimensional compressible Navier-Stokes equations for a perfect heat-conducting gas has been used for the purpose. The convective and viscous terms are discretized with a fifth-order weighted essentially non-oscillatory (WENO) scheme and a sixth-order central difference scheme, respectively. A three-stage, third-order Runge-Kutta scheme is adopted for time advancing. The convergence of all the flow statistics has been carefully checked. Flow stations at approximately the same value of the friction Reynolds number $Re_\tau \approx 420$ are hereafter considered for comparison, where $Re_\tau = \rho_w u_\tau \delta_{99}/\mu_w$ with ρ_w and μ_w denoting density and dynamic viscosity at the wall, δ_{99} the 99% boundary-layer thickness and u_τ the friction velocity.

Governing equations.—A full set of transport equations to describe energy exchanges in compressible turbulent flows is herein derived. The transport equations of mean kinetic energy and turbulence kinetic energy, namely $k_m = \frac{1}{2}\langle\rho\rangle\{u_i\}\{u_i\}$, $k_t = \frac{1}{2}\langle\rho u_i'' u_i''\rangle$, are widely acknowledged [19] and expressed as

$$\frac{\mathrm{D}k_m}{\mathrm{D}t} = -P_k + D_m + D_p^m + D_\nu^m - E + \Pi^m + \phi^{Mp} + \phi^{M\nu}, \tag{1}$$

$$\frac{\mathrm{D}k_t}{\mathrm{D}t} = P_k + D_t + D_p + D_\nu - \varepsilon + \Pi^p - \phi^{Mp} - \phi^{M\nu}, \tag{2}$$

*Electronic address: liweipeng@sjtu.edu.cn

where $\mathrm{D}\cdot/\mathrm{D}t = \partial\cdot/\partial t + \partial\cdot\{u_k\}/\partial x_k$. In (1), P_k accounts for production, D_m for mean-flow convection, D_p^m and D_ν^m account for pressure and viscous diffusion of k_m, respectively, E for mean viscous work, Π^m for mean pressure-dilatation, and ϕ^{Mp} and $\phi^{M\nu}$ are associated with pressure and viscous actions, respectively. In (2), the terms P_k, ϕ^{Mp} and $\phi^{M\nu}$ are the same as in (1), hence they are interpreted as yielding transfer energy between k_m and k_t; D_t is the turbulent convection, D_p and D_ν account for pressure and viscous diffusion of k_t, respectively, ε is the viscous dissipation, and Π^p is the so-called pressure-strain term [3].

These expressions of the various terms are as follows

$$
\begin{gathered}
P_k = -\left\langle \rho u_i'' u_k'' \right\rangle \frac{\partial\{u_i\}}{\partial x_k},\ D_m = -\frac{\partial\left\langle \rho u_i'' u_k'' \right\rangle\{u_i\}}{\partial x_k},\\
D_p^m = -\frac{\partial\langle p\rangle\langle u_i\rangle}{\partial x_i},\ D_\nu^m = \frac{\partial\langle \tau_{ik}\rangle\langle u_i\rangle}{\partial x_k},\\
E = \langle \tau_{ik}\rangle \frac{\partial\langle u_i\rangle}{\partial x_k},\ \Pi^m = \langle p\rangle \frac{\partial\langle u_i\rangle}{\partial x_i},\\
\phi^{Mp} = \langle u_i''\rangle \frac{\partial\langle p\rangle}{\partial x_i},\ \phi^{M\nu} = -\langle u_i''\rangle \frac{\partial\langle \tau_{ik}\rangle}{\partial x_k},\\
D_t = -\frac{1}{2}\frac{\partial\left\langle \rho u_i'' u_i'' u_k'' \right\rangle}{\partial x_k},\ D_p = -\frac{\partial\left\langle p' u_i'' \right\rangle}{\partial x_i},\\
D_\nu = \frac{\partial\left\langle \tau_{ik}' u_i'' \right\rangle}{\partial x_k},\ \varepsilon = \left\langle \tau_{ik}' \frac{\partial u_i''}{\partial x_k} \right\rangle,\ \Pi^p = \left\langle p' \frac{\partial u_i''}{\partial x_i} \right\rangle,
\end{gathered} \tag{3}
$$

where $\langle\cdot\rangle$ and $\{\cdot\}$ denote Reynolds- and Favre-averaging operators (e.g. for an arbitrary variable ξ, $\{\xi\} = \langle\rho\xi\rangle/\langle\rho\rangle$) respectively, and single and double primes denote fluctuations thereof. x_i $(i = 1, 2, 3)$ is used to denote the streamwise, wall-normal and spanwise direction, respectively, u_i denotes the corresponding velocity components, t is time, ρ is the fluid density, p is the pressure, and τ_{ij} is the viscous stress, expressed as $\mu[(\partial u_i/\partial x_j + \partial u_j/\partial x_i) - \frac{2}{3}\delta_{ij}\partial u_k/\partial x_k]$, with μ the dynamic viscosity and δ_{ij} the Kronecker delta.

In order to derive governing equations for mean and turbulence internal energy, we find it convenient to introduce a new diagnostic variable $\phi = (C_v T)^{1/2} = c/\left((\gamma-1)\gamma\right)^{1/2}$, where T is the absolute temperature, C_v is the specific heat at constant volume, γ is the specific heat ratio, and $c = (\gamma R T)^{1/2}$ is the sound speed. This formalism bears the clear advantage that the internal energy becomes $e = \rho\phi^2$, with obvious formal similarity with the expression of the turbulence kinetic energy $(k = 1/2\rho u_i^2)$, thus allowing to draw clearer similarities and differences in terms of the mechanisms underlying their exchanges. As a result of this definition, the expressions of the mean and turbulence internal energies are as follows, $e_m = \langle\rho\rangle\{\phi\}\{\phi\}$ and $e_t = \langle\rho\phi''\phi''\rangle$,

With $e = \rho\phi^2$, the energy equation is rewritten as

$$
\frac{\partial \rho\phi^2}{\partial t} + \frac{\partial \rho\phi^2 u_k}{\partial x_k} = -\frac{\partial q_k}{\partial x_k} - p\frac{\partial u_k}{\partial x_k} + \tau_{ij}\frac{\partial u_i}{\partial x_j}, \tag{4}
$$

where q_k is the heat flux vector. Let $f = -\partial q_k/\partial x_k - p\partial u_k/\partial x_k + \tau_{ij}\partial u_i/\partial x_j$, using mass conservation (4) can be reformulated as

$$
\frac{\partial \rho\phi}{\partial t} + \frac{\partial \rho u_k\phi}{\partial x_k} = \frac{f}{2\phi}. \tag{5}
$$

Applying the Reynolds averaging procedure to (5) yields

$$
\frac{\partial\langle\rho\rangle\{\phi\}}{\partial t} + \frac{\partial\langle\rho\rangle\{u_k\}\{\phi\}}{\partial x_k} + \frac{\partial\langle\rho u_k''\phi''\rangle}{\partial x_k} = \left\langle \frac{f}{2\phi} \right\rangle, \tag{6}
$$

which, making use of average mass balance yields

$$
\frac{\partial\{\phi\}}{\partial t} + \{u_k\}\frac{\partial\{\phi\}}{\partial x_k} + \frac{1}{\langle\rho\rangle}\frac{\partial\langle\rho u_k''\phi''\rangle}{\partial x_k} = \frac{1}{\langle\rho\rangle}\left\langle \frac{f}{2\phi} \right\rangle. \tag{7}
$$

With help of the ideal gas state equation $p = \rho R T$, pressure is replaced with $(\gamma-1)\rho\phi^2$, with its average value $\langle p\rangle$ split into mean and turbulent contributions, namely $\langle p_m\rangle = (\gamma-1)\langle\rho\rangle\{\phi\}\{\phi\}$, $\langle p_t\rangle = (\gamma-1)\langle\rho\phi''\phi''\rangle$.

Using $(\{\phi\}\cdot(6) + \langle\rho\rangle\{\phi\}\cdot(7))$, we obtain the transport equation for mean internal energy

$$
\frac{\mathrm{D}e_m}{\mathrm{D}t} = -P_e + D_e^m + Q - \Pi^{pm} + E + \varepsilon + \phi^{Tq} + \phi^{Td} + \phi^{T\nu}, \tag{8}
$$

where P_e accounts for turbulence internal energy production, D_e^m for convection of mean internal energy, Q for heat conduction, Π^{pm} is the mean flow contribution to pressure-dilatation, ϕ^{Tq}, ϕ^{Td} and $\phi^{T\nu}$ account for heat-conduction, velocity-dilatation and viscous actions due to temperature variation, respectively. E and ε are the same as those in (1) and (2), thus representing energy exchanges between mean internal energy and mean and turbulence kinetic energy, respectively. The expressions for the various terms in (8) are as follows

$$
\begin{gathered}
P_e = -2\left\langle \rho u_k''\phi''\right\rangle \tfrac{\partial\{\phi\}}{\partial x_k},\ D_e^m = -2\tfrac{\partial\left\langle \rho u_k''\phi''\right\rangle\{\phi\}}{\partial x_k},\\
Q = -\left\langle \tfrac{\partial q_k}{\partial x_k}\right\rangle,\ \Pi^{pm} = \left\langle p_m\right\rangle \tfrac{\partial\langle u_k\rangle}{\partial x_k},\ \phi^{Tq} = \left\langle \tfrac{\partial q_k}{\partial x_k}\tfrac{\phi''}{\phi}\right\rangle,\\
\phi^{Td} = (1-\gamma)\left\langle (\rho\phi)'\tfrac{\partial u_k''}{\partial x_k}\right\rangle,\ \phi^{T\nu} = -\left\langle \tau_{ij}\tfrac{\partial u_i}{\partial x_j}\tfrac{\phi''}{\phi}\right\rangle\{\phi\}.
\end{gathered}
\tag{9}
$$

By subtracting (7) from (5), a transport equation for fluctuation of ϕ is obtained,

$$
\begin{aligned}
&\frac{\partial\phi''}{\partial t} + u_k''\frac{\partial\phi''}{\partial x_k} + \{u_k\}\frac{\partial\phi''}{\partial x_k} + u_k''\frac{\partial\{\phi\}}{\partial x_k}\\
&-\frac{1}{\langle\rho\rangle}\frac{\partial\left\langle \rho u_k''\phi''\right\rangle}{\partial x_k} = \frac{1}{\rho}\left(\frac{f}{2\phi}\right)' - \left(\frac{1}{\langle\rho\rangle}-\frac{1}{\rho}\right)\left\langle\frac{f}{2\phi}\right\rangle,
\end{aligned}
\tag{10}
$$

which we recast in divergence form

$$
\begin{aligned}
&\frac{\partial\rho\phi''}{\partial t} + \frac{\partial\rho u_k''\phi''}{\partial x_k} + \frac{\partial\rho\{u_k\}\phi''}{\partial x_k} + \rho u_k''\frac{\partial\{\phi\}}{\partial x_k}\\
&-\frac{\rho}{\langle\rho\rangle}\frac{\partial\left\langle \rho u_k''\phi''\right\rangle}{\partial x_k} = \left(\frac{f}{2\phi}\right)' - \left(\frac{\rho}{\langle\rho\rangle}-1\right)\left\langle\frac{f}{2\phi}\right\rangle.
\end{aligned}
\tag{11}
$$

Similarly, by taking $\langle\rho\phi''\cdot(10)+\phi''\cdot(11)\rangle$, we obtain a transport equation for the turbulence internal energy

$$
\frac{\mathrm{D}e_t}{\mathrm{D}t} = P_e + D_e^t - \Pi^p - \Pi^{pt} - \phi^{Tq} - \phi^{Td} - \phi^{T\nu},
\tag{12}
$$

where P_e, ϕ^{Tq}, ϕ^{Td}, and $\phi^{T\nu}$ are common to (8), and Π^p is common to (2). Here, D_e^t denotes turbulent convection of e_t, Π^{pt} is the turbulent component of the pressure-dilatation, such that $\Pi^m = \Pi^{pm} + \Pi^{pt}$ (see (1), (8)),

$$
D_e^t = -\frac{\partial\left\langle \rho\phi''\phi'' u_k''\right\rangle}{\partial x_k} \text{ and } \Pi^{pt} = \langle p_t\rangle\frac{\partial\langle u_k\rangle}{\partial x_k}.
\tag{13}
$$

A similar attempt to derive evolution equations for mean and turbulence internal energy was made in the pioneering work of Mittal and Girimaji [2]. However, their derivation was based on introduction of a pressure-like variable (namely, $(p/(\gamma-1))^{1/2}$), rather than the sound-speed-based variable (ϕ) introduced in this study. As a consequence, given that the turbulence Mach number and pressure fluctuations are small also in hypersonic boundary layers, the budget terms in their pressure-based turbulence internal equations are vanishingly small as compared to the magnitude of the kinetic contributions [17]. This is not the case in the present formalism, with major advantage in terms of interpretation. Quantitative differences of the two approaches as regards the matching exchange terms will be referred to below.

The transport equations (1), (2), (8), (12), constitute a comprehensive framework for the study of energy exchanges between kinetic and internal energy modes, as expressed in their common terms. Note that the sum of these four equations consequently recovers the average of the total energy equation. The overall possible pathways for energy exchanges are outlined in figure 1. As one can see, the production terms of kinetic and internal energy (P_k and P_e) transfer energy from the mean flow field to the fluctuating field, with additional $k_m - k_t$ transfer terms associated with pressure work (ϕ^{Mp}) and viscous action (ϕ^{Mv}), and $e_m - e_t$ transfer terms associated with heat conduction (ϕ^{Tq}), velocity dilatation (ϕ^{Td}), and viscous action (ϕ^{Tv}). Energy exchanges between kinetic (k_m and k_t) and internal energy (e_m and e_t), are controlled by five interaction terms (E, Π^{pm}, Π^{pt}, ε and Π^p). Based on the sketch reported in figure 1, we now proceed to examine all possible routes of energy exchange by mining the DNS database.

Results and discussion.— The energy exchanges are quantified on the basis of equations (1), (2), (8), (12), with the spatial derivatives calculated by a second-order central difference of the corresponding DNS data for the internal grid points and the order of accuracy reduces to first order at the boundaries. Balance of each equation is well achieved, reconfirming the accuracy of the derived transport equations.

The distributions of exchange terms are hereafter reported in wall units, namely using the friction velocity $u_\tau = (\tau_w/\rho_w)^{1/2}$ as velocity scale, and $\delta_v = \mu_w/(\rho_w u_\tau)$ as length scale, where τ_w is the wall friction. Wall units are hereafter denoted with the + superscript. This classical representation has been retained here, although alternative

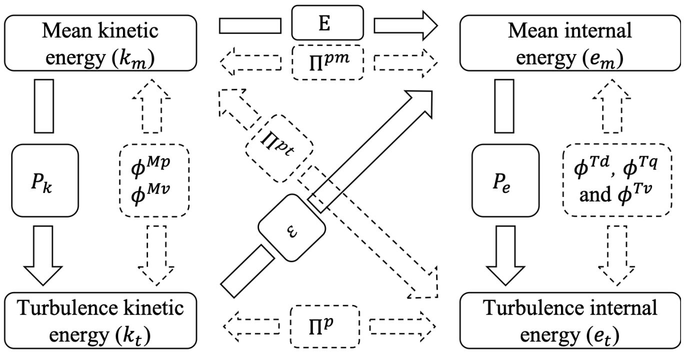

FIG. 1: Pathways for energy exchanges among mean and turbulence kinetic and internal energy. Solid arrows denote one-way exchanges, while dashed arrows denote two-way (reversible) exchanges.

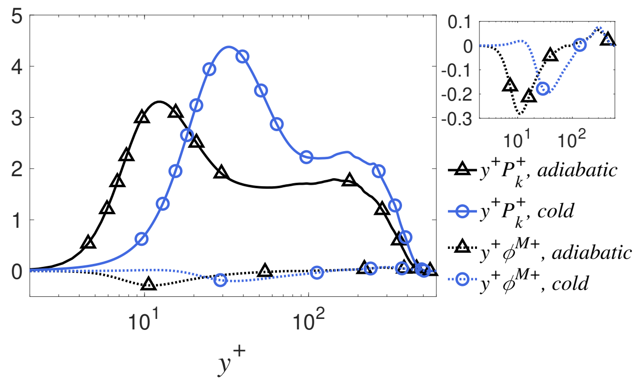

FIG. 2: $k_m - k_t$ exchanges: profiles of turbulence kinetic energy production and sum of pressure and viscous action associated with density variation.

scalings [e.g. 9, 14] can yield greater universality of the distributions. Furthermore, the distributions of all quantities as a function of the inner-scales wall distance (y^+) are shown in semi-logarithmic scale, and in pre-multiplied form (namely, each term is multiplied by y^+), in such a way that equal areas underneath the graphs correspond to equal integrated contributions.

(*a*) $k_m - k_t$ exchanges: The energy transfer between k_m and k_t is determined by terms P_k, ϕ^{Mp} and ϕ^{Mv}. Their profiles are shown in figure 2. Positive value of the P_k^+ term throughout the wall layer suggests that, in agreement with classical interpretation, production withdraws energy from the mean flow field to feed turbulent fluctuations. Under adiabatic wall conditions (black lines), a large amount of energy is transferred in the inner region ($y^+ < 30$), with a primary peak at $y^+ \approx 12$. A secondary peak is also present in the outer region, peaking at $y^+ \approx 200$, signifying the generation of large-scale energy-containing turbulent motions [20, 21]. In the presence of wall cooling (blue lines), the peaks of $y^+P_k^+$ become higher, as a direct result of mean thermodynamic properties variation, the influence of which would be eliminated with application of a semi-local normalization [9], and the primary peak moves away from the wall (in terms of wall units), whereas the second peak is barely affected. This result confirms that inner- to outer-layer separation tends to be reduced from wall cooling [22].

The pressure work term ϕ^{Mp} and the viscous term ϕ^{Mv} are due to difference of Reynolds and Favre averages, as a result of density variations. Since their magnitudes are 1–2 orders smaller than P_k, their sum is plotted in figure 2. This is found to be negative in the inner region and positive in the outer region under adiabatic wall condition. However, when the wall is cooled, positive values are also found in the near-wall region, indicating energy transfer from k_t to k_m. This switch is related to the change of sign of the net mass flux, $\langle u_i'' \rangle$.

(*b*) $e_m - e_t$ exchanges: Figure 3 shows profiles of P_e, ϕ^{Td}, ϕ^{Tq} and ϕ^{Tv}, which determine energy transfer between e_m and e_t. In figure 3, P_e^+ is large and it remains positive across the whole boundary layer, indicating that internal production withdraws energy from e_m to e_t. This observation is physically reasonable, but quite different from what is found in a pressure-based framework [2], in which the values of internal production are negligible and somehow negative, even at Mach number as high as eight [17]. Different from P_k^+, a prominent peak of P_e^+ is observed in the outer region, which is mitigated by wall cooling. To explain this feature, we have checked the variations of two terms

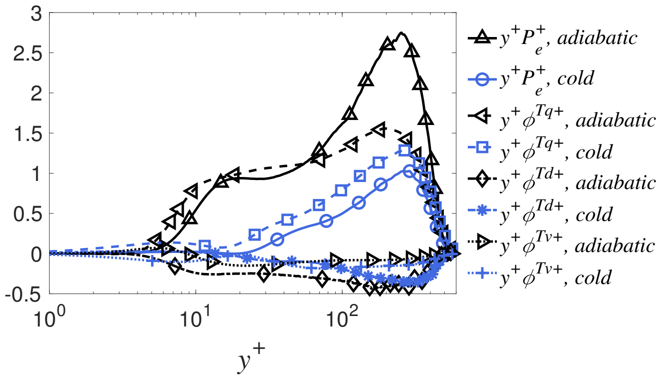

FIG. 3: $e_m - e_t$ exchanges: profiles of turbulence internal energy production, heat-conduction, velocity-dilatation and viscous action associated with temperature variation.

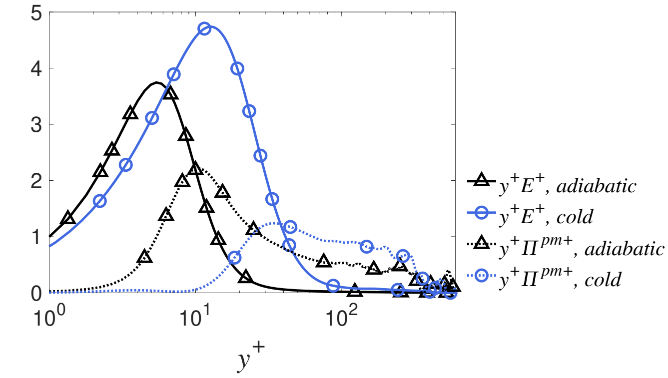

FIG. 4: $k_m - e_m$ exchanges: profiles of mean viscous work and mean-flow pressure-dilatation.

contributing to P_e, namely $\partial\{\phi\}/\partial y$ and $\langle \rho u_2'' \phi'' \rangle$, which account for the wall-normal conductive and turbulent heat flux, respectively. We find that generation of P_e in the outer layer is primarily related to turbulent heat flux, whose reduction in the cold case causes P_e attenuation (not shown). Since the wall-normal motions from higher-temperature to lower-temperature regions communicate positive ϕ fluctuations [23], these two terms are always opposite in sign, in such a way that P_e stays positive throughout the wall layer, regardless of the wall conditions.

The heat conduction term ϕ^{Tq} is found to mainly transfer energy from e_t to e_m, whereas the velocity dilatation term ϕ^{Td} plays a competing role. In the presence of wall cooling, both terms are weakened, except in the viscous sublayer (say, $y^+ < 5$), where heat conduction is relatively dominant. In contrast, viscous work ϕ^{Tv} yields slight redistribution of energy from e_t to e_m for $y^+ < 9$, with reversal at larger wall distance, in the adiabatic case. With wall cooling, this term always draws energy from mean flow to turbulence. In general, we find that wall cooling introduces remarkable modification of the energy transfer mechanisms in the very-near-wall region.

(*c*) $k_m - e_m$ exchanges: Two factors, namely mean viscous work E and mean flow contribution to pressure-dilatation Π^{pm}, control the energy exchange between k_m and e_m, as depicted in figure 4. Both terms withdraw energy from k_m to e_m, primarily in the inner wall layer. Wall cooling shifts their peaks farther from the wall, with the E^+ peak increasing, and the Π^{pm+} peak decreasing. The energy transfer via Π^{pm} vanishes near the wall, and it tends to be more concentrated in the outer region at $T_w/T_r = 0.25$, which is mainly associated with the variation of $\partial \langle u_k \rangle / \partial x_k$ (see (9)).

(*d*) $k_m - e_t$ exchanges: The turbulent contribution to mean pressure-dilatation Π^{pt} transfers energy from e_t to k_m. Its profile is not shown as its magnitude is very small, and it can be safely ignored, at least at the Mach number and wall temperatures under scrutiny.

(*e*) $k_t - e_m$ exchanges: The viscous dissipation ε converts turbulence kinetic energy into heat [24]. Its profile is shown in figure 5, which clarifies that wall cooling enhances transfer significantly. The viscous dissipation ε can be split into contributions along the streamwise, wall-normal and spanwise directions, namely $\varepsilon_{ii} = \langle \tau'_{ik} \partial u_i'' / \partial x_k \rangle, i = 1, 2, 3$. Figure 5 shows that the streamwise contribution ε_{11} dominates over the others, and all contributions are amplified

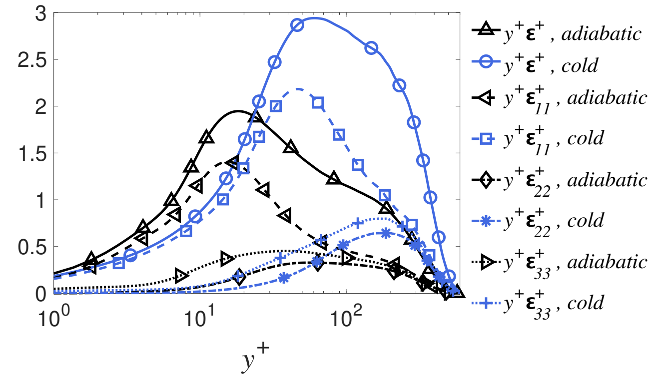

FIG. 5: $k_t - e_m$ exchanges: profiles of viscous dissipation and its contributions along the streamwise, wall-normal, and spanwise directions.

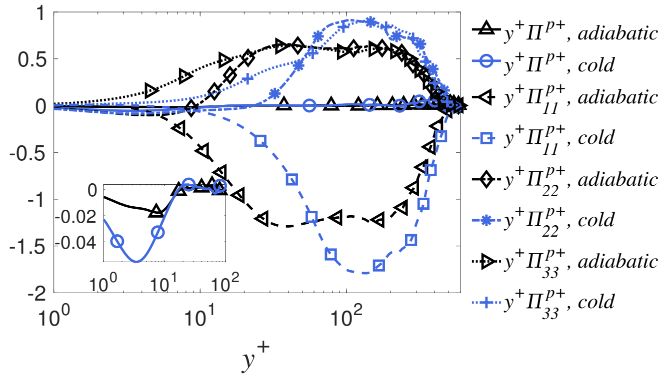

FIG. 6: $k_t - e_t$ exchanges: profiles of pressure-strain term and its contributions along the streamwise, wall-normal, and spanwise directions.

and shifted away from the wall by wall cooling.

(*f*) $k_t - e_t$ exchanges: The interaction between k_t and e_t is controlled by the pressure-strain term Π^p, as displayed in figure 6. This term is exclusive to compressible flows owing to non-zero dilatation, and it has been applied as an explicit indicator to measure genuine compressibility effects [25]. Pressure-strain is mainly confined to $y^+ < 10$, converting k_t into e_t. When the wall is cooled, higher values of Π^p are observed, which corroborates the idea that wall cooling promotes compressibility effects, consistent with observation made by Duan et al. [11] and Chu et al. [26]. Nonetheless, its magnitude is still quite small, as its integrated value throughout the boundary layer is less than 2% of the energy transfer from k_m to k_t.

Similar to viscous dissipation, the pressure-strain term can be split into components associated with coordinate directions, namely $\Pi^p_{ii} = \langle p' \partial u''_i / \partial x_i \rangle, i = 1, 2, 3$, which act to exchange energy between different velocity components, and whose profiles are shown in figure 6. Negative values of Π^p_{11} and positive values of Π^p_{22} and Π^p_{33} suggest that energy is primarily transfered from $k_{t,1}$ to $k_{t,2}$ and $k_{t,3}$ (here, $k_{t,i} = 1/2 \langle \rho u''_i u''_i \rangle, i = 1, 2, 3$). Due to wall impermeability, $y^+\Pi^{p+}_{22}$ is negative near the wall, and it mainly redistributes $k_{t,2}$ to $k_{t,3}$, owing to the effect of quasi-streamwise vortices [5]. Wall cooling causes the energy exchange to take place farther from the wall in terms of y^+, and the peak magnitude to increase.

Summary.—In this letter, we have presented a novel theoretical framework to analyze energy exchanges in compressible flows, which we have used to analyze the effects of wall cooling in hypersonic turbulent boundary layers, based on a high-fidelity numerical database. Formulation of suitable transport equations for mean and turbulent contributions to kinetic and internal energy leads us to clearly identify multiple routes of energy exchange, as outlined in figure 1. Especially meaningful in this respect is the formulation of the internal energy transport equations in terms of a sound-speed-like variable, which has the clear advantage of yielding full structural similarity with the kinetic energy transport equations, thus allowing to illuminate more neatly the mechanisms of energy exchange. For the specific case of hypersonic turbulent boundary layers, we find dominant energy interactions to be production (P_k in $k_m - k_t$ and P_e in $e_m - e_t$), heat conduction (Φ^{Tq} in $e_m - e_t$), mean pressure-dilatation (Π^{pm} in $k_m - e_m$), and dissipation (E

in $k_m - e_m$ and ε in $k_t - e_m$). The occurrence of wall cooling yields significant variations in energy exchanges, with common tendency for leading mechanisms to take place farther from the wall, in terms of wall units. We anticipate that the formalism herein established can facilitate more systematic and in-depth studies on compressible flows within an energetic framework, not limited to the case of wall-bounded flows which we have considered as an example. We also expect that the present study can help the development of physics-informed models for compressible turbulence in the class of RANS (Reynolds-averaged Navier-Stokes) [27], and LES (large-eddy-simulation) [28], which currently heavily hinge on variable-density extrapolation of their incompressible counterparts.

This study was supported by Grant No. 92052101 and 91952302 from National Natural Science Foundation of China.

[1] D. S. Praturi and S. S. Girimaji. Effect of pressure-dilatation on energy spectrum evolution in compressible turbulence. *Phys. Fluids*, 31(5):055114, 2019.
[2] A. Mittal and S. S. Girimaji. Mathematical framework for analysis of internal energy dynamics and spectral distribution in compressible turbulent flows. *Phys. Rev. Fluids*, 4:042601(R), Apr 2019.
[3] S. Arun, A. Sameen, B. Srinivasan, and S. S. Girimaji. Scale-space energy density function transport equation for compressible inhomogeneous turbulent flows. *J. Fluid Mech.*, 920:A31, 2021.
[4] T. Kawata and P. H. Alfredsson. Inverse interscale transport of the Reynolds shear stress in plane couette turbulence. *Phys. Rev. Lett.*, 120:244501, Jun 2018.
[5] M. Lee and R. D. Moser. Spectral analysis of the budget equation in turbulent channel flows at high reynolds number. *J. Fluid Mech.*, 860:886–938, 2019.
[6] D. H. Richter. Turbulence modification by inertial particles and its influence on the spectral energy budget in planar couette flow. *Phys. Fluids*, 27(6):063304, 2015.
[7] M. P. Martin. Direct numerical simulation of hypersonic turbulent boundary layers. Part 1. Initialization and comparison with experiments. *J. Fluid Mech.*, 570:347–364, 2007.
[8] C. Zhang, L. Duan, and M. M. Choudhari. Effect of wall cooling on boundary-layer-induced pressure fluctuations at mach 6. *J. Fluid Mech.*, 822:5–30, 2017.
[9] C. Zhang, L. Duan, and M. M. Choudhari. Direct numerical simulation database for supersonic and hypersonic turbulent boundary layers. *AIAA J.*, 56(11):4297–4311, 2018.
[10] M. Yu and C.-X. Xu. Compressibility effects on hypersonic turbulent channel flow with cold walls. *Phys. Fluids*, 33(7): 075106, 2021.
[11] L Duan, I Beekman, and MP Martin. Direct numerical simulation of hypersonic turbulent boundary layers. Part 2. Effect of wall temperature. *J. Fluid Mech.*, 655:419–445, 2010.
[12] L. Duan, I. Beekman, and M. P. Martin. Direct numerical simulation of hypersonic turbulent boundary layers. Part 3. Effect of mach number. *J. Fluid Mech.*, 672:245–267, 2011.
[13] M. V. Morkovin. Effects of compressibility on turbulent flows. *Mécanique de la Turbulence*, 367:380, 1962.
[14] Y.-S. Zhang, W.-T. Bi, F. Hussain, X.-L. Li, and Z.-S. She. Mach-number-invariant mean-velocity profile of compressible turbulent boundary layers. *Phys. Rev. Lett.*, 109:054502, Jul 2012.
[15] Y.-S. Zhang, W.-T. Bi, F. Hussain, and Z.-S. She. A generalized Reynolds analogy for compressible wall-bounded turbulent flows. *J. Fluid Mech.*, 739:392–420, 2014.
[16] K. P. Griffin, L. Fu, and P. Moin. Velocity transformation for compressible wall-bounded turbulent flows with and without heat transfer. *P. Natl. Acad. Sci. USA*, 118(34), 2021. ISSN 0027-8424.
[17] D.-H. Xu, J.-C. Wang, M.-P. Wan, C.-P. Yu, X.-L. Li, and S.-Y. Chen. Compressibility effect in hypersonic boundary layer with isothermal wall condition. *Phys. Rev. Fluids*, 6:054609, May 2021.
[18] M. Bernardini, D. Modesti, F. Salvadore, and S. Pirozzoli. Streams: A high-fidelity accelerated solver for direct numerical simulation of compressible turbulent flows. *Comput. Phys. Commun.*, 263:107906, 2021. ISSN 0010-4655.
[19] S. Pirozzoli, F. Grasso, and T. B. Gatski. Direct numerical simulation and analysis of a spatially evolving supersonic turbulent boundary layer at M=2.25. *Phys. Fluids*, 16(3):530–545, 2004.
[20] Y. Hwang and C. Cossu. Self-sustained process at large scales in turbulent channel flow. *Phys. Rev. Lett.*, 105:044505, Jul 2010.
[21] A. Cimarelli, E. De Angelis, and C. M. Casciola. Paths of energy in turbulent channel flows. *J. Fluid Mech.*, 715:436–451, 2013.
[22] J. Huang, L. Duan, and M. M. Choudhari. Direct numerical simulation of hypersonic turbulent boundary layers: effect of spatial evolution and Reynolds number. *J. Fluid Mech.*, 937:A3, 2022.
[23] S. Pirozzoli and M. Bernardini. Turbulence in supersonic boundary layers at moderate reynolds number. *J. Fluid Mech.*, 688:120–168, 2011.
[24] R. M. McMullen, M. C. Krygier, J. R. Torczynski, and M. A. Gallis. Navier-Stokes equations do not describe the smallest scales of turbulence in gases. *Phys. Rev. Lett.*, 128:114501, Mar 2022.
[25] S. K. Lele. Compressibility effects on turbulence. *Annu. Rev. Fluid Mech.*, 26(1):211–254, 1994.
[26] Y.-B. Chu, Y.-Q. Zhuang, and X.-Y. Lu. Effect of wall temperature on hypersonic turbulent boundary layer. *J. Turbul.*, 14(12):37–57, 2013.

[27] Yildirim Suzen and Klaus Hoffmann. *Investigation of supersonic jet exhaust flow by one- and two-equation turbulence models.* 1998.

[28] G. Erlebacher, M. Y. Hussaini, C. G. Speziale, and T. A. Zang. Toward the large-eddy simulation of compressible turbulent flows. *J. Fluid Mech.*, 238:155–185, 1992.